Dynamic Sensorless Detection of Linear Electromagnetic UAV Launch

Guangjun Tan, Baoquan Kou, *Member, IEEE*, Hongxing Wu, and Liyi Li, *Member, IEEE*

***Abstract*—The technical solution of Unmanned Aerial Vehicle (UAV) has the following features: good controllability; simple thrust control; high precision; long operating life; low cost; strong adaptability, repeatability, maneuverability, and imperceptibility. So the UAV has widespread application prospects. The position sensor of the mover of UAV linear electromagnetic ejection is the key component of control system. It has a direct influence on performance, structure, and reliability of the system. As the sensors such as linear photoelectric encoder and magnetic encoder are not able to meet the demand of high speed control, the paper develops the research on the detection methods of the mover position. First, the paper presents a detection method of mover position based on sliding mode observer. Due to the flicker problem of sliding mode observer, the paper then proposes a detection method based on state observer, and the method can result in smooth detected position of the mover. Finally, the simulated results of the ejection verify the validity of the proposed method.**

***Index Terms*—Ejection, permanent magnet linear synchronous motor (PMLSM), sensorless, sliding mode observer (SMO), state observer.**

I. Introduction

NOWADAYS, UAV plays a very important role in modern wars, and it has more widespread application prospects for civil use. High resolution linear scales are commonly employed to function as sensors to detect mover position in the system of UAV Electromagnetic Ejection. However, the introduction of position sensor may bring in some problems. As the motion length of the ejection is 4 meters long, the installation and maintenance of the position sensor are difficult, and the existence of position sensor may deteriorate the reliability and increase the complexity of the system operation. Besides, the response speed of the linear scales in the market at present cannot meet the demand of high speed detection of the system operation. So it is of great significance to study the sensorless detection technology of the mover position of the ejection.

For detection of the mover position of the ejection, the sensorless detection technology must satisfy the following two requirements: its algorithm is simple and is feasible in actual application; it can implement accurate detection of the position in real time, whether the ejection is under accelerating starting condition or high speed operation. There exist several methods in current sensorless detection research. The most popular methods include sliding mode observer (SMO) method [1]–[5], model reference adaptive control (MRAC) [6], extended Kalman filter (EKF) method [7], [8], assumed rotary coordinate method [9]–[11], high frequency signal injection method, and artificial intelligence methods (fuzzy control and neural networks control). However, MRAC, EKF, and artificial intelligence methods need a large amount of calculation, and these methods are not suitable for practical application. The assumed rotary coordinate method is effective only if the mover is running at a stable operating state, and may result in failures at accelerating starting process. The high frequency signal injection method is only suitable for salient PMSM.

Based on the requirements of sensorless detection for ejection, and the shortages of the aforementioned methods, the paper selects the SMO method as one of the detection methods. The SMO method is a relatively novel detection method, which uses bang-bang control theory to achieve fast tracking performance. The method has good robustness, and can response to the mover speed immediately. However, as sliding mode observer method, in essence, is discontinuous switch control, which easily brings in system flicker, the paper designs another method based on state observer in comparison with the SMO method. Through simulation experiments, we can analyze and judge the advantages of the two methods, and determine to choose the final design solution. The experimental electromagnetic launcher and its control system are shown in Figs. 1 and 2.

II. Mathematical Model of Electromagnetic Ejection

The motor employed in the Electromagnetic ejection is a surface mounted permanent magnet linear synchronous motor (PMLSM). The voltage equation of its stator windings in the stationary $\alpha\beta$ coordinate system is

$$\frac{d\boldsymbol{i_s}}{dt} = A\boldsymbol{i_s} + B(\boldsymbol{u_s} - \boldsymbol{e_s}) \tag{1}$$

where

$$\boldsymbol{i_s} = [\, i_\alpha \quad i_\beta \,]^T \quad \boldsymbol{u_s} = [\, u_\alpha \quad u_\beta \,]^T$$
$$\boldsymbol{e_s} = [\, e_\alpha \quad e_\beta \,]^T = \frac{\pi v}{\tau}\psi_f\,[\, -\sin\tfrac{\pi s}{\tau} \quad \cos\tfrac{\pi s}{\tau} \,]^T$$
$$A = \begin{bmatrix} -\frac{R}{L} & 0 \\ 0 & -\frac{R}{L} \end{bmatrix} \quad B = \begin{bmatrix} \frac{1}{L} & 0 \\ 0 & \frac{1}{L} \end{bmatrix}$$

τ is the polar pitch of the mover, v is the linear speed of the mover, and s is the linear displacement of the mover.

Manuscript received January 11, 2010; revised February 28, 2010; accepted March 21, 2010. Date of publication April 26, 2010; date of current version January 7, 2011. This work was supported in part by the Natural Science Foundation of China under Grant 50877012 and in part by the Program for New Century Excellent Talents of China in University under Grant NCET-06-0336.

The authors are with the Electrical Engineering Department, Harbin Institute of Technology, Harbin 150001, China (e-mail: tangjtangj@126.com; koubq@hit.edu.cn; whx0422@sina.com.cn; liliyi.hit@gmail.com).

Color versions of one or more of the figures in this paper are available online at http://ieeexplore.ieee.org.

Digital Object Identifier 10.1109/TPS.2010.2046915

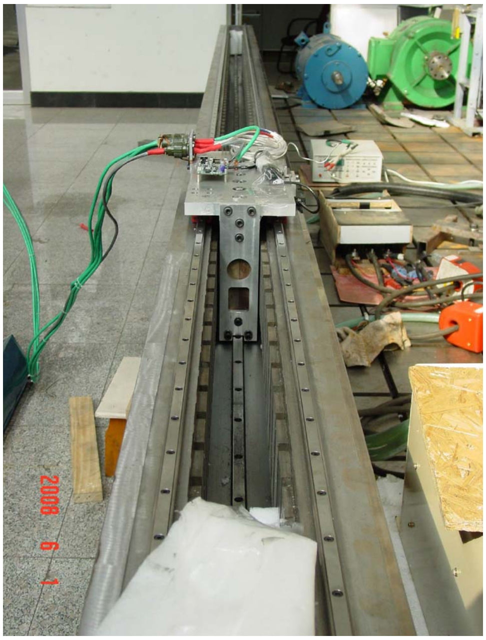

Fig. 1. Experimental electromagnetic launcher.

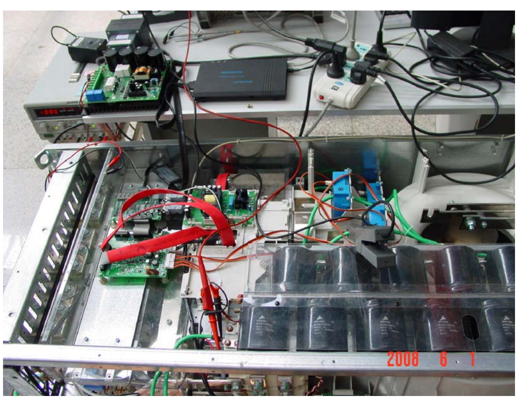

Fig. 2. Inner structure of the control system for the electromagnetic launcher.

III. Design of the SMO Method

A. Model of the SMO

According to the state equations of the motor, under the premise that the stator terminal voltage and the stator armature current can be obtained, respectively by voltage and current sensors, the SMO model constructed to estimate the stator EMF can be expressed by the following equations:

$$\begin{cases} \frac{d\widetilde{\boldsymbol{i}}_{\boldsymbol{s}}}{dt} = A\widetilde{\boldsymbol{i}}_{\boldsymbol{s}} + B(\boldsymbol{u}_{\boldsymbol{s}} - h\widetilde{\boldsymbol{e}}_{\boldsymbol{s}} - \boldsymbol{z}) \\ \boldsymbol{z} = k \cdot \operatorname{sgn}(\widetilde{\boldsymbol{i}}_{\boldsymbol{s}} - \boldsymbol{i}_{\boldsymbol{s}}) \\ \frac{d\widetilde{\boldsymbol{e}}_{\boldsymbol{s}}}{dt} = -\omega_0 \widetilde{e}_s + \omega_0 \boldsymbol{z} \end{cases} \tag{2}$$

where, $\widetilde{\boldsymbol{i}}_{\boldsymbol{s}}$ and $\widetilde{\boldsymbol{e}}_{\boldsymbol{s}}$ are respectively the observed stator armature current and the observed stator EMF. k is the observer gain, h is the feedback gain $(h > -1)$, and ω_0 is the cutoff frequency of the first-order low-pass filter. The structure of the SMO method is shown in Fig. 3.

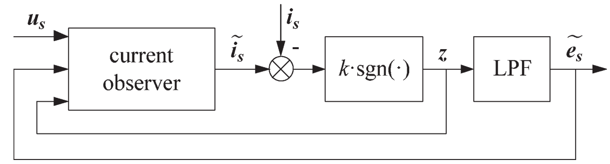

Fig. 3. Sliding mode observer of the stator EMF.

B. Stability Analysis of the SMO

First we should demonstrate the stability of the SMO method. If we define the observed error of stator armature current as $\widehat{\boldsymbol{i}}_{\boldsymbol{s}} = \widetilde{\boldsymbol{i}}_{\boldsymbol{s}} - \boldsymbol{i}_{\boldsymbol{s}}$, then the dynamic equation about the current observed error $\widehat{\boldsymbol{i}}_{\boldsymbol{s}}$ can be derived from (1) and (2) as follows:

$$\frac{d\widehat{\boldsymbol{i}}_{\boldsymbol{s}}}{dt} = A\widehat{\boldsymbol{i}}_{\boldsymbol{s}} + B(\boldsymbol{e}_{\boldsymbol{s}} - h\widetilde{\boldsymbol{e}}_{\boldsymbol{s}} - \boldsymbol{z}). \tag{3}$$

If we define the sliding mode surface of the observer is $\boldsymbol{S} = \widehat{\boldsymbol{i}}_{\boldsymbol{s}} = \widetilde{\boldsymbol{i}}_{\boldsymbol{s}} - \boldsymbol{i}_{\boldsymbol{s}} = 0$, and select the function $V = (1/2)\boldsymbol{S}^T\boldsymbol{S}$ as the Lyapunov function of the observer, which is positive other than equal to zero at origin. The condition for the observer to achieve global asymptotic stability is

$$\frac{dV}{dt} = \boldsymbol{S}^T \frac{d\boldsymbol{S}}{dt} < 0. \tag{4}$$

Substituting (3) into (4), and ignoring the impact of the stator armature resistance, equation (4) can be expressed at $\alpha\beta$ coordinate system as follows:

$$\frac{1}{L}\left[\widehat{i}_\alpha(e_\alpha - h\widetilde{e_\alpha} - k\operatorname{sgn}\widehat{i}_\alpha) + \widehat{i}_\beta(e_\beta - h\widetilde{e_\beta} - k\operatorname{sgn}\widehat{i}_\beta)\right] - \frac{R}{L}\left(\widehat{i}_\alpha^{\,2} + \widehat{i}_\beta^{\,2}\right) < 0. \tag{5}$$

In order to calculate the value of the observer gain k, we need to work out the relationship among all the electrical quantities first of all. As the linear speed of the mover is v, we can assume that the low-frequency component of the z signal is

$$\boldsymbol{z}_{eq} = Z\cos\frac{\pi v t}{\tau}. \tag{6}$$

In order to facilitate the analysis, here the phase angle of $\boldsymbol{z}_{eq}$ is assumed as 0, which has no effect on the result of the analysis. Through the LPF, $\boldsymbol{z}$ signal is turned into $\widetilde{e}_s$, and by computation, $\widetilde{e}_s$ is derived as

$$\widetilde{e}_s = \frac{\omega_0 Z}{\omega_0^2 + \left(\frac{\pi v}{\tau}\right)^2}\left(\omega_0\cos\frac{\pi v t}{\tau} + \frac{\pi v}{\tau}\sin\frac{\pi v t}{\tau}\right). \tag{7}$$

As the SMO method takes small-amplitude switching movement along the sliding surface, $\widehat{\boldsymbol{i}}_{\boldsymbol{s}} = 0$ is held approximately right, so the actual stator EMF $\boldsymbol{e}_s$ is

$$\begin{aligned} \boldsymbol{e}_{\boldsymbol{s}} &= h\widetilde{\boldsymbol{e}}_{\boldsymbol{s}} + \boldsymbol{z}_{eq} \\ &= \frac{h\omega_0 Z}{\omega_0^2 + \left(\frac{\pi v}{\tau}\right)^2}\left(\omega_0\cos\frac{\pi v t}{\tau} + \frac{\pi v}{\tau}\sin\frac{\pi v t}{\tau}\right) + Z\cos\frac{\pi v t}{\tau} \\ &= \frac{h\omega_0 Z}{\omega_0^2 + \left(\frac{\pi v}{\tau}\right)^2}\left[\frac{(h+1)\omega_0^2 + \left(\frac{\pi v}{\tau}\right)^2}{h\omega_0}\cos\frac{\pi v t}{\tau} + \frac{\pi v}{\tau}\sin\frac{\pi v t}{\tau}\right]. \end{aligned} \tag{8}$$

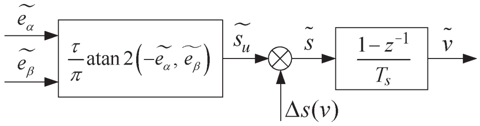

Fig. 4. Position and linear speed estimation schematic.

According to (1), it is learned that the amplitude of actual stator EMF $\boldsymbol{e}_s$ is $\pi\psi_f v/\tau$, so we can get that

$$\frac{\pi\psi_f v}{\tau} = \frac{h\omega_0 Z}{\omega_0^2 + \left(\frac{\pi v}{\tau}\right)^2}\sqrt{\left[\frac{(h+1)\omega_0^2 + \left(\frac{\pi v}{\tau}\right)^2}{h\omega_0}\right]^2 + \left(\frac{\pi v}{\tau}\right)^2}. \tag{9}$$

Through (9), Z, the amplitude of $\boldsymbol{z}_{eq}$, is deduced as

$$Z = \frac{\pi\psi_f v\left[\omega_0^2 + \left(\frac{\pi v}{\tau}\right)^2\right]}{h\tau\omega_0\sqrt{\left[\frac{(h+1)\omega_0^2 + \left(\frac{\pi v}{\tau}\right)^2}{h\omega_0}\right]^2 + \left(\frac{\pi v}{\tau}\right)^2}}. \tag{10}$$

In order to ensure the SMO can operate stably, the observer gain k should satisfy

$$\begin{aligned} k &> \max(e_\alpha - h\widetilde{e_\alpha}, e_\beta - h\widetilde{e_\beta}) \\ &= \frac{\pi\psi_f v\left[\omega_0^2 + \left(\frac{\pi v}{\tau}\right)^2\right]}{\tau\sqrt{\left[\omega_0^2(h+1) + \left(\frac{\pi v}{\tau}\right)^2\right]^2 + \left(\frac{\pi h\omega_0 v}{\tau}\right)^2}}. \end{aligned} \tag{11}$$

C. Displacement Compensation for the SMO

Due to the low-pass filter is set at the end of the sliding mode observer, the observed EMF will certainly lags behind the actual EMF, so a position compensation algorithm is needed to compensate for the displacement lag $\Delta s(v)$, which is caused by the sliding mode observer. From (7) and (8), we can obtain both the phase angles of $\boldsymbol{e}_s$ and $\widetilde{\boldsymbol{e}_s}$. The displacement lag $\Delta s(v)$ can be expressed as the difference between the two phase angles, and then to be multiplied by the coefficient τ/π

$$\begin{aligned} \Delta s(v) &= \frac{\tau}{\pi}\left\{\arctan\frac{\pi v}{\omega_0\tau} - \arctan\frac{\pi h\omega_0 v}{\left[(h+1)\omega_0^2 + \left(\frac{\pi v}{\tau}\right)^2\right]\tau}\right\} \\ &= \frac{\tau}{\pi}\arctan\frac{\pi v}{(h+1)\omega_0\tau}. \end{aligned} \tag{12}$$

To obtain the information of the mover position, it is commonly adopted to do trigonometric function $(\operatorname{atan2}(\cdot,\cdot))$ computation with the observed EMF, and the predicted position $\widetilde{s_u}$ can be calculated as

$$\widetilde{s_u} = \frac{\tau}{\pi}\operatorname{atan}2(-\widetilde{e_\alpha}, \widetilde{e_\beta}). \tag{13}$$

Then, adding the displacement lag $\Delta s(v)$ to the predicted position $\widetilde{s_u}$, the final estimated position $\widetilde{s}$ is derived. The estimated linear speed $\widetilde{v}$ can be obtained by difference computing of $\widetilde{s}$. The implementation schematic is shown in Fig. 4.

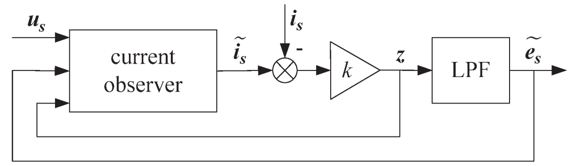

Fig. 5. State observer of the stator EMF.

IV. Design of the State Observer Method

A. Shortages of the SMO Method

As the SMO method is apt to bring in flicker problem when the mover is under high speed operation, an improved SMO method is to displace the signum function $(\operatorname{sgn}(\cdot))$ by the symmetric saturating linear transfer function $(\operatorname{satlins}(\cdot))$ [1], [3] or the hyperbolic tangent sigmoid function $(\operatorname{sigmoid}(\cdot))$ [4], [5]. This improvement can eliminate the flicker problem in observing position. However, if the current observed error $\widehat{\boldsymbol{i}_s}$ is so small that it does not reach the saturation regions of the satlins or sigmoid functions, this improved method cannot make sure that the SMO method takes small-amplitude switching movement along the sliding surface, so the premise $\widehat{\boldsymbol{i_s}} = 0$ is not held right. Therefore, (12) is not valid to calculate the displacement lag $\Delta s(v)$, which is due to the nonlinear property of the satlins and the sigmoid functions.

B. Model of the State Observer

In order to solve the nonlinear problem of the improved SMO method, a detection method based on state observer is introduced here. The state observer is one kind of purely linear observer, and all the signals used in the observer are sinusoidal signals, so the displacement lag $\Delta s(v)$ can be calculated accurately. The state observer model constructed to estimate the stator EMF can be expressed by the following equations:

$$\begin{cases} \frac{d\widetilde{\boldsymbol{i_s}}}{dt} = A\widetilde{\boldsymbol{i_s}} + B(\boldsymbol{u_s} - h\widetilde{\boldsymbol{e_s}} - \boldsymbol{z}) \\ \boldsymbol{z} = k(\widetilde{\boldsymbol{i_s}} - \boldsymbol{i_s}) \\ \frac{d\widetilde{\boldsymbol{e_s}}}{dt} = -\omega_0\widetilde{\boldsymbol{e_s}} + \omega_0\boldsymbol{z}. \end{cases} \tag{14}$$

The structure of the state observer method is shown in Fig. 5.

From the state observer model, it is clearly seen that the difference between the SMO method and the state observer method is just the definition of $\boldsymbol{z}$. In the SMO method, $\boldsymbol{z}$ signal is defined as the signum function of $\widehat{\boldsymbol{i}_s}$, while it is defined as the linear function of $\widehat{\boldsymbol{i}_s}$ in the state observer method.

C. Displacement Compensation for the State Observer

The displacement lag in the state observer method is caused not just by the LFP, but the current observer represented by the first equation of (14). The total displacement lag is the sum of these two lag.

According to (1) and (14), the dynamic equation about the current observed error $\widehat{\boldsymbol{i_s}}$ can be expressed as

$$\frac{d\widehat{\boldsymbol{i_s}}}{dt} = A\widehat{\boldsymbol{i_s}} + B(\boldsymbol{e_s} - h\widetilde{\boldsymbol{e_s}} - \boldsymbol{z}). \tag{15}$$

As z signal is continuous, we can assume that z signal is

$$\boldsymbol{z} = Z\cos\frac{\pi v t}{\tau}. \tag{16}$$

Through the LPF, $\boldsymbol{z}$ signal is turned into $\widetilde{\boldsymbol{e}_s}$, and by computation, $\widetilde{\boldsymbol{e}_s}$ is derived as

$$\widetilde{\boldsymbol{e_s}} = \frac{\omega_0 Z}{\omega_0^2 + \left(\frac{\pi v}{\tau}\right)^2}\left(\omega_0\cos\frac{\pi v t}{\tau} + \frac{\pi v}{\tau}\sin\frac{\pi v t}{\tau}\right). \tag{17}$$

As $z = k(\widetilde{\boldsymbol{i}_s} - \boldsymbol{i}_s) = k\widehat{\boldsymbol{i}_s}$, the observed current error $\widehat{\boldsymbol{i}_s}$ can be expressed as

$$\widehat{\boldsymbol{i_s}} = \frac{\boldsymbol{z}}{k} = \frac{Z}{k}\cos\frac{\pi v t}{\tau}. \tag{18}$$

Substituting (16)–(18) into (15), we have

$$\begin{aligned} -\frac{\pi Z v}{k\tau}\sin\frac{\pi v t}{\tau} = -\frac{ZR}{kL}\cos\frac{\pi v t}{\tau} + \frac{1}{L}\Bigg[\boldsymbol{e_s} - Z\cos\frac{\pi v t}{\tau} \\ - \frac{h\omega_0 Z}{\omega_0^2 + \left(\frac{\pi v}{\tau}\right)^2}\left(\omega_0\cos\frac{\pi v t}{\tau} + \frac{\pi v}{\tau}\sin\frac{\pi v t}{\tau}\right)\Bigg]. \end{aligned} \tag{19}$$

So the actual stator EMF $\boldsymbol{e}_s$ is

$$\begin{aligned} \boldsymbol{e_s} = Z\Bigg\{\left[1 + \frac{R}{k} + \frac{h\omega_0^2}{\omega_0^2 + \left(\frac{\pi v}{\tau}\right)^2}\right]\cos\frac{\pi v t}{\tau} \\ + \left[\frac{\pi h\omega_0 v}{\tau\left[\omega_0^2 + \left(\frac{\pi v}{\tau}\right)^2\right]} - \frac{\pi L v}{k\tau}\right]\sin\frac{\pi v t}{\tau}\Bigg\}. \end{aligned} \tag{20}$$

From (20) and (17), we can obtain both the phase angles of $\boldsymbol{e}_s$ and $\widetilde{\boldsymbol{e}_s}$. The displacement lag $\Delta s(v)$ can be expressed as the difference between the two phase angles, and then to be multiplied by the coefficient τ/π

$$\begin{aligned} \Delta s(v) &= \frac{\tau}{\pi}\left\{\arctan\frac{\pi v}{\omega_0\tau} - \arctan\frac{\frac{\pi h\omega_0 v}{\tau\left[\omega_0^2 + \left(\frac{\pi v}{\tau}\right)^2\right]} - \frac{\pi L v}{k\tau}}{1 + \frac{R}{k} + \frac{h\omega_0^2}{\omega_0^2 + \left(\frac{\pi v}{\tau}\right)^2}}\right\} \\ &= \frac{\tau}{\pi}\arctan\frac{\pi\tau v\left(k + R + \omega_0 L\right)}{\omega_0\tau^2\left[(h+1)k + R\right] - \pi^2 L v^2}. \end{aligned} \tag{21}$$

The implementation schematic is shown in Fig. 4., which is the same as that of the SMO method.

V. Simulation Experiments

The parameters of the ejection are shown in Table I.

The ejection accelerates from zero speed to 25 m/s at the maximum acceleration. The ejection is under speed open loop control from zero speed to 1.2 m/s, and then under speed closed loop control, respectively, switching to SMO method and state observer method. The simulation results are shown in Figs. 6 and 7. In the figures, the blue curve represents the actual position of the mover, and the red curve represents the observed position of the mover.

From the figures above, it is clearly seen that, no matter whether the mover is under starting progress or under high speed operation, the flicker problem still exists in the position observation by using the SMO method, which can be eliminated

TABLE I
System Parameters of the Ejection

Symbol	Item	Value
m	mass of the mover	30kg
M	mass of additional matter	50kg
f_s	switching frequency	8kHz
τ	polar pitch	0.06m
F_{max}	maximum thrust	800N
k_F	thrust constant	22.40N/A
v_{max}	outlet velocity	25m/s
U_{dc}	DC input voltage	850V
R	stator armature resistance	0.073Ω
L	stator armature inductance	0.499mH
k_{SMO}	SMO gain	1050
k_{state}	state observer gain	20
h	feedback gain	1
ω_0	cut-off frequency of LPF	200rad/s

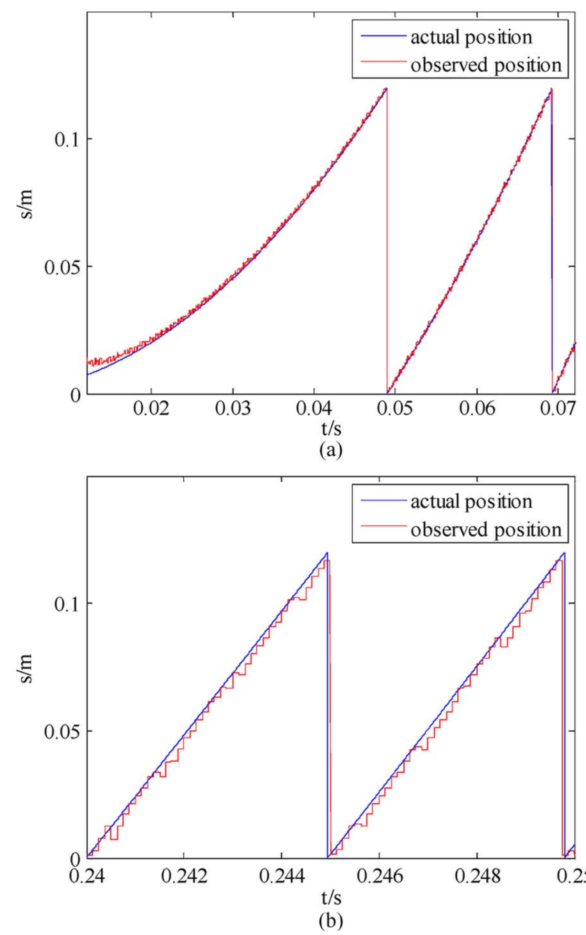

Fig. 6. Curves of actual and observed position by SMO method (a) Accelerating starting progress (b) High speed operation.

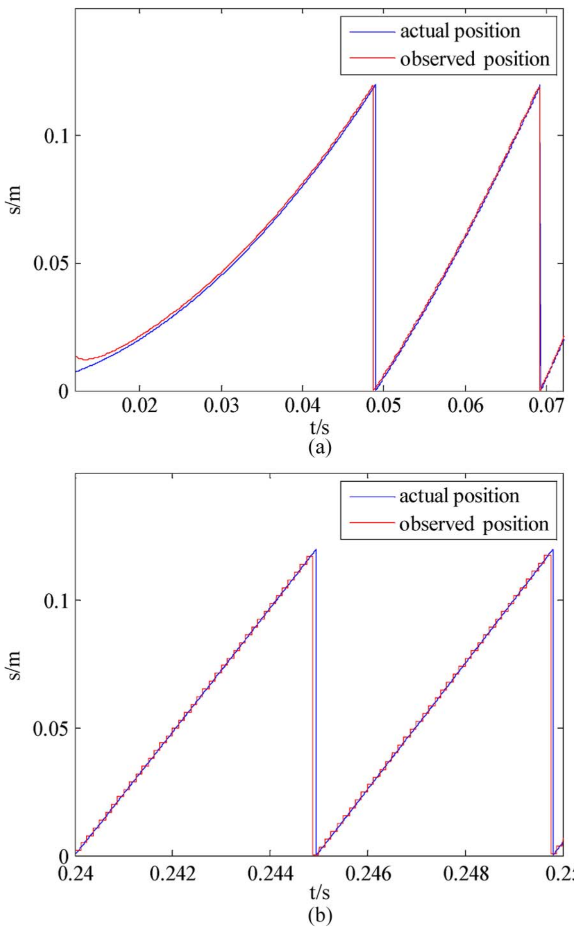

Fig. 7. Curves of actual and observed position by state observer method (a) Accelerating starting progress (b) High speed operation.

by using the state observer method. The position compensation algorithms are both adopted in the SMO and state observer method, so the observed position can track well with the actual position in these two methods. Based on the above analysis, it is known that the state observer method is a better choice than SMO method in observing the mover position of the ejection.

VI. Conclusion

The paper first designs the SMO method for ejection, and proposes a displacement compensation algorithm to solve the displacement lagging problem due to low-pass filter. As the sliding mode observer method is apt to bring in flicker problem, a pure linear state observer method is proposed in the paper, and the displacement compensation algorithm for the method is adopted as well. Through the results derived from simulation experiments, it is easily found that, by comparison with the SMO method, the state observer method can detect more accurately the mover position of the electromagnetic ejection. Furthermore, the state observer method can eliminate the flicker problem, which exists in the SMO method. The executive cycle of the state observer algorithm implementation is short, so it is a better solution as a detection method to be applied in high speed operation.

References

[1] S. Chi, Z. Zhang, and L. Xu, “Sliding-mode sensorless control of direct-drive PM synchronous motors for washing machine applications,” *IEEE Trans. Ind. Appl.*, vol. 45, no. 2, pp. 582–590, Mar./Apr. 2009.

[2] Y.-S. Han, J.-S. Choi, and Y.-S. Kim, “Sensorless PMSM drive with a sliding mode control based adaptive speed and stator resistance estimator,” *IEEE Trans. Magn.*, vol. 36, no. 5, pp. 3588–3591, Sep. 2000.

[3] L. Wenqi, H. Yuwen, H. Wenxin, C. Jianbo, D. Xuyang, and Y. Jianfei, “Sensorless control of permanent magnet synchronous machine based on a novel sliding mode observer,” in *Proc. IEEE Vehicle Power Propulsion Conf.*, Harbin, China, Sep. 3–5, 2008, pp. 1–4.

[4] K. Paponpen and M. Konghirun, “An improved sliding mode observer for speed sensorless vector control drive of PMSM,” in *Proc. Power Electron. Motion Control Conf.*, Aug. 14–16, 2006, vol. 2, pp. 1–5.

[5] W. Eom, I. Kang, and J. Lee, “Enhancement of the speed response of PMSM sensorless control using an improved adaptive sliding mode observer,” in *Proc. 34th IEEE Annu. Conf. Ind. Electron.*, Nov. 10–13, 2008, pp. 188–191.

[6] M. Rashed, P. F. A. MacConnell, A. F. Stronach, and P. Acarnley, “Sensorless indirect-rotor-field-orientation speed control of a permanent-magnet synchronous motor with stator-resistance estimation,” *IEEE Trans. Ind. Electron.*, vol. 54, no. 3, pp. 1664–1675, Jun. 2007.

[7] M. Boussak, “Implementation and experimental investigation of sensorless speed control with initial rotor position estimation for interior permanent magnet synchronous motor drive,” *IEEE Trans. Power Electron.*, vol. 20, no. 6, pp. 1413–1422, Nov. 2005.

[8] S. Bolognani, M. Zigliotto, and M. Zordan, “Extended-range PMSM sensorless speed drive based on stochastic filtering,” *IEEE Trans. Power Electron.*, vol. 16, no. 1, pp. 110–117, Jan. 2001.

[9] B.-H. Bae, S.-K. Sul, J.-H. Kwon, and J.-S. Byeon, “Implementation of sensorless vector control for super-high-speed PMSM of turbo-compressor,” *IEEE Trans. Ind. Appl.*, vol. 39, no. 3, pp. 811–818, May/Jun. 2003.

[10] B. Nahid-Mobarakeh, F. Meibody-Tabar, and F.-M. Sargos, “Back EMF estimation-based sensorless control of PMSM: Robustness with respect to measurement errors and inverter irregularities,” *IEEE Trans. Ind. Appl.*, vol. 43, no. 2, pp. 485–494, Mar./Apr. 2007.

[11] B. Nahid-Mobarakeh, F. Meibody-Tabar, and F.-M. Sargos, “Mechanical sensorless control of PMSM with online estimation of stator resistance,” *IEEE Trans. Ind. Appl.*, vol. 40, no. 2, pp. 457–471, Mar./Apr. 2004.

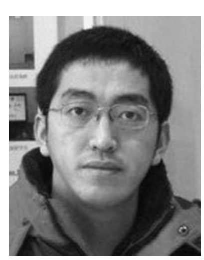

Guangjun Tan received the B.E. and M.E. degrees from Harbin Institute of Technology, Harbin, China, in 2006 and 2008, respectively. He is currently with the Institute of Electromagnetic and Electronic Technology, Harbin Institute of Technology, as a doctoral candidate from 2008.

His research areas are sensorless control and drive of high-speed, low-inductance PMSM.

Baoquan Kou (M’09) received the B.E. and D.E. degrees from Harbin Institute of Technology, Harbin, China, in 1992 and 2004, respectively, and the M.E. degree from Chiba Institute of Technology, Chiba, Japan, in 1995.

He has been working in the mobile station for the post-doctors of HIT from 2005. From 2007, He is the professor in the School of Electrical Engineering and Automation, HIT. His research areas are electric drive of electric vehicle, linear motor and linear electromagnetic drive, control of the power quality, and superconducting motor.

Hongxing Wu received the B.E., M.E., and D.E. degrees from Harbin Institute of Technology, Harbin, China, in 1998, 2000, and 2005, respectively.

From 2006, he is a post-doctorate in the post-doctoral workstation of Guangzhou Hitachi Elevator Company, Guangzhou. From 2007, He is the associate professor in the School of Electrical Engineering and Automation, HIT. His research areas are the control and drive of motor, control and communication of electric vehicle, engineering control and simulation software, and linear thrust and linear launch.

Liyi Li (M'09) received the B.E., M.E., and D.E. degrees from Harbin Institute of Technology, Harbin, China, in 1991, 1995, and 2001, respectively.

From 1991 to 1993, he worked in the Science And Technology Development General Company of HIT. From 2002 to 2004, he worked in the mobile station for the post-doctors of Dalian University of Technology, Dalian, China. From 2004, He is the professor in the School of Electrical Engineering and Automation, HIT. His research areas are control and drive of linear electromagnetic system, linear electromagnetic launch, accumulation of electric energy, and superconducting motor.